MODELING INTERACTIONS OF FLOW AND VEGETATION FOR IMPROVED RIVERINE SYSTEM MANAGEMENT

Daniel Dombroski, Hydraulic Engineer, BOR, Denver TSC, CO, ddombroski@usbr.gov; Blair Greimann, Hydraulic Engineer, BOR, Denver TSC, CO; Yong Lai, Hydraulic Engineer, BOR, Denver TSC, CO; Victor Huang, Hydraulic Engineer, BOR, Denver TSC, CO; Lisa Fotherby, Hydraulic Engineer, BOR, Denver TSC, CO; Mark Stone, Assistant Professor, UNM Dept. Civil Eng., NM; Li Chen, Associate Research Professor, DRI Division of Hydrologic Sciences, NV

Abstract: The establishment, growth, and decline of riparian vegetation within impacted riverine systems is a growing challenge due to the increasing priority of maintaining ecosystem function while sustaining water supply and providing flood protection. A quantitative two-dimensional model is presented for predicting the interactions between flow and vegetation that is currently under development at BOR. The model is based upon the SRH-2D package, which contains a two-dimensional flow and mobile bed sediment transport model. The new SRH-2DV package incorporates a module that simulates the effect of vegetation on river and floodplain hydraulics through spatially distributed roughness. The coupled vegetation-hydraulic solver uses measured vegetation parameters to calculate a spatially-distributed, dynamic Manning's roughness coefficient while simulating the hydrodynamics of the system. Field and modeling work focused on a reach of the San Joaquin River near Fresno, California. Simulation results using the vegetation module are compared with measured water surface elevation and results from a manually-calibrated SRH-2D hydraulics model. We present initial simulation results from application to simple case studies and discuss the utility of expanding the predictive capabilities for application within more complex systems. Results from SRH-2DV will aid the science, economics, and policy of establishing environmental flows by addressing questions regarding the physical interaction of flow and vegetation in rivers and floodplains.

INTRODUCTION

The survival of riparian vegetation within managed river systems is a growing challenge due to the increasing priority of maintaining or restoring ecosystem function while balancing the need for water supply and flood protection. Riparian vegetation plays many important roles in the hydraulic, geomorphic, and ecologic processes of river systems (Naiman, 2010; Gurnell 2014). The ecological services provided by riparian vegetation are beneficial to both the river system and the human population surrounding the system (Groffman et al., 2003). Examples of these services include soil retention (Waters 1995), water quality improvement (Barling and Moore 1994), nutrient cycling (Dahm *et al*. 2002; Hill 1996), habitat provisioning (Keller *et al*. 1993; Stauffer and Best 1980), and flood damage mitigation (Brauman *et al*. 2007). The ecological services associated with riparian areas have been severely degraded in many river systems as the result of river engineering, floodplain development, and watershed development (Sweeney et al., 2004).

At the local scale, riparian vegetation increases flood risk by reducing effective flow areas and increasing hydraulic roughness (Rhee et al., 2008; Wilson et al, 2005; Green 2005). Reducing flow resistance in areas sensitive to flooding has historically been performed by vegetation removal (Darby, 1999; Masterman and Thorne 1992). At the watershed scale, however, vegetation-induced roughness has been

shown to enhance flood wave attenuation (Anderson 2006). Properly characterizing hydraulic roughness at the local scale is important for understanding hydrodynamic heterogeneity at the reach scale, including velocity and shear stress distributions and momentum exchange (Vermaas et al., 2011; Proust et al., 2013; Stone and Hotchkiss, 2007).

Vegetation resists flow due to drag forces on discrete elements and nonlinear interactions between multiple elements (Nepf, 2012). Flow resistance in natural systems is often characterized through the estimation of a dimensionless (e.g., Darcy friction factor f) or dimensional (e.g., Chezy coefficient C and Manning's n) roughness parameter that is used to model the hydraulics. Roughness parameters derive from a combination of empiricism and hydrodynamic theory and are generally interrelated deterministically. The roughness of a vegetated channel is generally a function of both the characteristics of the vegetation (e.g., size, density, flexibility, leaf area) and the flow (depth and velocity; due to streamlining effects). For computational convenience, however, roughness has historically been assumed independent of hydraulic conditions. Chow (1959) produced a list of bracketed roughness values corresponding to various vegetated flow types. Thompson & Roberson (1976) presented an analytical method for predicting roughness due to a flow through vegetation modeled as rigid or flexible cylinders. The method depends on estimation of a drag coefficient, stem spacing and diameter, and flexural rigidity. Kouwen & Li (1980) developed an iterative approach for calculating roughness as a function of vegetation rigidity, and estimated plant deflection in response to forcing exerted by the flow. The Kouwen & Li (1980) approach is generally applicable to grasses, and the authors provid a table with stiffness values for a large variety of grass types. Kouwen & Fathi-Moghadam (2000) describe methodology to estimate resistance due to coniferous trees in open-channel flow by modifying a previously existing model (Fathi-Moghadam & Kouwen, 1997) in order to account for variations in the flexibility between species. The authors obtained species-specific parameters for the equations by conducting intricate laboratory and field experiments to measure drag force on model trees. Darby (1999) presents a simplified cross-section based model for predicting roughness associated with sediment or vegetation. The approach applies one of six different empirically calibrated flow resistance equations at each computational node. An equation similar to the Kouwen & Li (1980) approach is used for flexible vegetation, while an equation similar to the Thompson & Roberson (1976) approach is used for nonflexible vegetation. A procedure for estimating roughness due to flow through stiff or flexible woody vegetation is described by Jarvela (2004). The method, limited to emergent vegetation, incorporates leaf area index (LAI) to account for the effect of leaf distribution on drag resistance. The author also presents (Jarvela, 2005) an analysis of flow structure over submerged flexible vegetation with a focus on velocity profiles and turbulence characteristics. Baptist et al. (2007) derive a Chezy-type formulation for calculating resistance due to submerged or emergent vegetation. The representative resistance coefficient includes contributions from the bed roughness, form drag from flow through the vegetation, and shear due to the velocity profile above the vegetation. Hession and Curran (2013) provide a literature review of trends and research in the topic of vegetation-induced roughness in fluvial systems; the authors discuss the spatio-temporal complexity of processes related to vegetation-flow-sediment interactions. Abu-Aly et al. (2014) present the results of two-dimensional hydraulic modeling using roughness derived from LiDAR. The authors demonstrate the effects of spatially-distributed roughness on hydraulics at the local and reach scale, and underscore the importance of systematically defining roughness at the resolution of the computational grid. The challenge of capturing the complexity of effects due to flow through a broad

range of vegetation types is reflected by the diversity of predictive methods developed during more than five decades of research.

Described herein is a deterministic computational tool for dynamically modeling spatially-distributed flow and vegetation interactions. An existing two-dimensional hydraulic and sediment transport model (SRH-2D) developed at the Bureau of Reclamation (BOR) Technical Service Center (TSC) is used as a basis for the new model development (SRH-2DV). The new SRH-2DV package iteratively computes hydraulic roughness due to vegetated flow as a function of the local hydraulics and vegetation characteristics. The algorithms and parameters applied are drawn from a combination of published literature and collaborative research. Results from SRH-2DV will aid the science, economics, and policy regarding riparian ecosystems by addressing uncertainties such as what impact riparian vegetation has on local flood conditions, how vegetation can be incorporated into restoration projects without increasing flood risks, and how management actions may impact habitat for endangered and threatened species.

METHODS

Model Development: The existing SRH-2D flow solver (Lai, 2010) is used as the computational base for the new SRH-2DV coupled flow and vegetation model. Hydraulic variables are computed by solving the depth-averaged dynamic wave equations using a finite volume numerical method. Solutions can be computed over an unstructured hybrid mesh (Lai, 1997; 2000), and the solver includes a seamless wetting-drying algorithm that is applied at each time step. With appropriate boundary conditions, constant or varying discharge flows may be simulated. The solver can compute subcritical and supercritical flow conditions without special treatment.

Bed shear stresses τ_{bx} and τ_{by} are calculated by the SRH-2D hydraulic solver using the Manning's roughness equation as follows:

$$\begin{pmatrix}\tau_{bx}\\ \tau_{by}\end{pmatrix} = \rho C_f \begin{pmatrix}U_x\\ U_y\end{pmatrix}\sqrt{U_x^2 + U_y^2}; \quad C_f = \frac{gn^2}{h^{1/3}} \tag{1}$$

where ρ is water density, U_x and U_y are the x and y velocity components, g is gravity, h is flow depth, and n is the Manning's roughness coefficient. The user-specified Manning's n is generally spatially-distributed yet independent of the computed hydraulic variables, and is a primary "tuning" parameter used during model calibration.

In the SRH-2DV vegetation model, the solver was modified to calculate dynamic Manning's n values at each cell in the computational mesh due to vegetated flow. The approaches of Baptist et al. (2007) and Järvelä (2004) were implemented in the model; the required input parameters could readily be measured in the field and applied within the modeling framework. Additional methods can be built into the modeling framework based on availability of supporting field data and will be investigated in future research.

The Järvelä (2004) approach is valid for emergent, stiff and flexible woody vegetation. The authors proposed the following equation to calculate the friction factor f,

$$f = 4C_{dX}\mathrm{LAI}\left(\frac{U}{U_X}\right)^X \frac{h}{H} \tag{2}$$

where $C_{d\chi}$ is a species-specific drag coefficient, LAI is leaf area index (defined as one-sided leaf area to projected ground surface ratio), U is the flow velocity magnitude, U_χ is a reference velocity (set to 0.1 m/s for this study), and χ is a species-specific exponent (set to -0.57 for this study). The ratio of h (water depth) over H (plant height) is a scaling factor to account for partial submergence ($h<H$). The parameters LAI and H are measured in the field as described below. The variable flow velocity and water depth are obtained from the coupled hydraulic solver, where U is calculated as the resultant of the horizontal velocity components at each mesh cell. The value of the drag parameter $C_{d\chi}$ was based on prior work done by Fathi-Moghadam (1996) and then varied on a species-specific basis in order to calibrate the model response. Thus the friction factor is a function of spatial variation in the plant parameters and spatial and temporal variation in the hydraulic variables. In practice, the Manning's n is used by the hydraulic solver (Equation 1) and is computed from the friction factor as

$$n = h^{\frac{1}{6}}\sqrt{\frac{f}{8g}} \tag{3}$$

Roughness can alternatively be calculated using the Baptist (2007) approach according to

$$C_r = \sqrt{\frac{1}{(1/C_b^2) + (C_d mDH/2g)}} + \frac{\sqrt{g}}{\kappa}\ln\left(\frac{h}{H}\right) \tag{4}$$

where C_b is the Chezy bed coefficient, C_d is the drag coefficient, m is plant density, D is stem diameter, H is plant height, κ = 0.41 is the von Karman constant, and h is the flow depth. Thus the composite resistance coefficient C_r includes the effects of bed resistance, form drag of flow through the vegetation, and the boundary layer formed above the vegetation. For emergent vegetation, the logarithmic term in Equation 4 is dropped since the resistance is only a function of the bed roughness and vegetative form drag. For dense vegetation, the contribution of the bed roughness term may be considered insignificant compared to the contribution of the vegetative drag term (C_b =80 for this study). The water depth h is obtained from the coupled hydraulic solver and the parameters m, D, and H are measured in the field. The drag coefficient C_d was initially set to unity (Baptist, et al., 2007) and then varied on a species-specific basis in order to calibrate the model response. The resistance in Equation 4 is converted to Manning's n as

$$n = \frac{1}{C_r}h^{1/6} \tag{5}$$

<u>Study Reach</u>: The SRH-2DV vegetation model was tested by simulating the hydraulics in a reach of the San Joaquin River west of Fresno, California located between Friant Dam and the Chowchilla Bifurcation structure. This section was selected due to the presence of diverse riparian vegetation types and the availability of pre-existing field data.

Floodplain vegetation in the study reach was classified by Moise and Hendrickson (2002) to have 30 different dominant vegetation classes (Holland, 1986). To further classify woody types, Moise and Hendrickson added a numerical value from 1 to 6 indicating branch density (high to low) based on Hink and Omhart's work (1984). Moise and Hendrickson (2002) found eleven classes that covered 92% of the vegetated area within the study reach: (1) cottonwood riparian of branch density 3; (2) cottonwood riparian low density of branch density 4; (3) and (4) herbaceous, mixed riparian of branch densities 1 and 3; (5) mixed riparian low density of branch density 6; (6) riparian scrub; (7) and (8) willow riparian of branch densities 3 and 4; (9) and (10) willow scrub of branch densities 5 and 6; and (11) willow scrub low density of branch density 6. The vegetation classifications were compiled into a GIS shapefile comprised of polygons delineating the spatial extent of the dominant classes within the study reach.

A computational mesh with boundary conditions was available for the reach from previous hydraulic modeling in support of the San Joaquin River Restoration Project (Dombroski, Greimann, & Gordon, 2012). The existing model was calibrated by comparing simulated water surface elevation to measured water surface elevation at a similar discharge. The Manning's *n* was then manually adjusted in the channel and floodplain areas in order to bring the simulated water surface elevation in better agreement with the measurements. Manually adjusting the Manning's *n* in order to effect the water surface elevation is generally successful in reproducing the gross effect of bed and form roughness; however, the approach includes no explicit treatment of roughness due to vegetation, which limits the capability of the model in predicting vegetative effects.

Empirical Data and Field Work: Development and testing of the SRH-2DV vegetation model was dependent on data reconnaissance in support of the parameterized physical processes. A field study was conducted (Gillihan, 2013) at six 1000 ft^2 sites along the San Joaquin River, producing measurements of vegetation height, stem diameter, stem density, and leaf area index. Vegetation height and stem diameter was measured with a hypsometer (Nikon Forestry Pro Laser) and caliper, respectively. LAI was measured using a photosynthetically active radiation (PAR) sensor (Decagon AccuPAR model LP-80). The field measurement sites were selected as representative samples of the dominant vegetation classes identified by Moise and Hendrickson (2002); the measured vegetation parameters were then applied to all instances of the delineated vegetation classes within the shapefile. An attribute table was constructed to contain the input data required to parameterize the model for each vegetation classification. The shapefile in conjunction with the attribute table defines the spatial distribution of vegetation and corresponding parameters throughout the study reach. The shapefile and attribute table are read directly by the SRH-2DV model and the vegetation information is mapped to the computational mesh over which the hydraulic variables are solved.

Table 1 and Table 2 contain a summary of the parameter values and sources used in the Jarvela (2004) and Baptist (2007) approaches, respectively. Values listed as Variable generally may depend on vegetation class and location, and are used to tune the model response during calibration. Values listed as Measured were taken from the results of the field campaign, and Dynamic indicates quantities calculated by the hydraulic solver that may vary in space and time. The values of fixed parameters are given with reference to a source in the published literature.

For regions within the computational mesh where a vegetation-based roughness was not applicable (e.g., in-channel, no-grow, and anthropogenically disturbed areas) or not physically reasonable, a static value of n=0.035 was assigned by default.

Table 1 Identification of parameters used in the Jarvela (2004) approach for computing hydraulic roughness.

Parameter	Value	Source
C_{dX}	Variable	Model Calibration
X	-0.57	Aberle & Jarvela, 2013
U_x	0.1 m/s (0.328 ft/s)	Aberle & Jarvela, 2013
LAI	Measured	Gillihan, 2013
H	Measured	Gillihan, 2013
U	Dynamic	Hydraulic Solver
h	Dynamic	Hydraulic Solver

Table 2 Identification of parameters used in the Baptist (2007) approach for computing hydraulic roughness.

Parameter	Value	Source
C_D	Variable	Model Calibration
C_b	80	Gillihan, 2013
m	Measured	Gillihan, 2013
D	Measured	Gillihan, 2013
H	Measured	Gillihan, 2013
h	Dynamic	Hydraulic Solver

RESULTS

The SRH-2DV vegetated flow solver was tested by simulating the hydraulics within a reach of the San Joaquin River at flow rates Q = 1100 (31), 2500 (71), 4000 (113), and 7500 (212) cfs (cms). The capability of the hydraulic roughness module in estimating roughness due to vegetation was evaluated by comparing computed Manning's n to manually calibrated Manning's n and by comparing computed water surface elevation to measured water surface elevation at a similar discharge. Also available for comparison is simulated water surface elevation from the manually calibrated model (Dombroski, Greimann, & Gordon, 2012). Figures 1 and 2 show comparisons of water surface elevation results using the Baptist (2007) approach and Jarvela (2004) approach for calculating hydraulic roughness due to vegetation. Also shown is water surface elevation from a simulation using manually calibrated roughness and field measurements of water surface elevation for a similar discharge. The results indicate that the Jarvela (2004) approach, although resulting in under predicted water surface elevation, performs better than the Baptist (2007) approach, and compares favorably with the performance of the manually calibrated model for large extents of the model reach.

The simulated water surface elevation is in part determined by the distribution of Manning's n values computed by the model for each vegetation type. Compiled in Figure 3 and 4 are distributions of

Manning's *n* values for well-represented vegetation types in the modeled reach of the San Joaquin River. The distributions are compiled from the Manning's *n* value at each cell in the computational mesh as designated by the vegetation type polygons. The distributions shown in each figure include (A) the calculated values for wetted cells using the Jarvela (2004) approach, (B) the polygon values including those calculated in wet cells and the default value of *n*=0.035 in dry cells, and (C) the values taken from the manually calibrated model. Also shown in each plot are the mean (solid line) and standard deviation from the mean (dashed line) of the calculated Manning's *n* values for wetted cells. The distribution of calculated Manning's *n* values (blue) in each plot is representative of cells that are directly coupled to the hydraulics through Equation 2. For Mixed Riparian (Figure 3) and Willow Riparian (Figure 4) vegetation types, the compilation of Manning's *n* values are approximately normally distributed around the mean value. Manning's *n* values calculated for the Willow Scrub (not shown) vegetation type do not appear to be normally distributed, possibly due to species-specific parameters that are causing the calculated roughness values to be biased low. The cumulative count of a distribution of Manning's *n* values provides an indication of the relative influence a given vegetation type has in the hydraulic computations the model is performing. The gross effects of vegetative roughness in the hydraulic model will be driven by vegetation types that are largely inundated for the flow simulated. In the model reach of the San Joaquin River, many cells within the computational mesh are classified as Agricultural Field. The count of calculated Manning's values is far less, however, indicating that the portion of inundated agricultural field (and therefore the effect of agricultural vegetation on the hydraulics within the reach) is small.

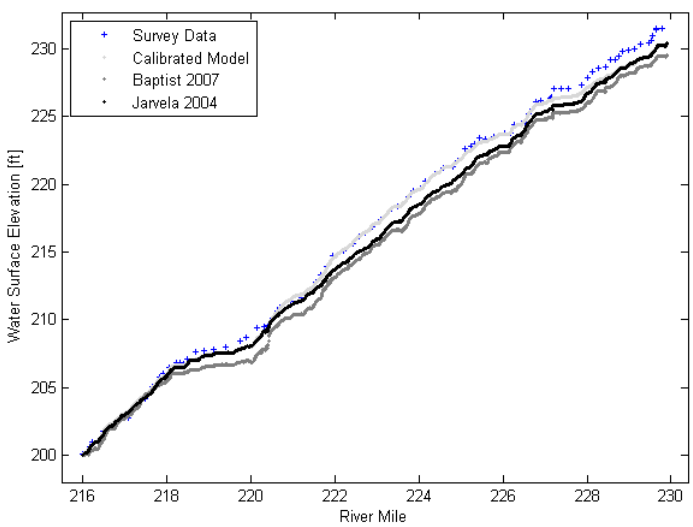

Figure 1 Simulated water surface elevation (ft) as a function of river mile (mi) for Q = 4000 cfs in a reach of the San Joaquin River. Shown for comparison are measured water surface elevation (blue), manually calibrated simulation results (light grey), simulation results using the Baptist (2007) approach (grey), and simulation results using the Jarvela (2004) approach (black). The figure demonstrates that the Jarvela (2004) approach performs better than the Baptist (2007) approach, although falls short of the performance of the manually calibrated model.

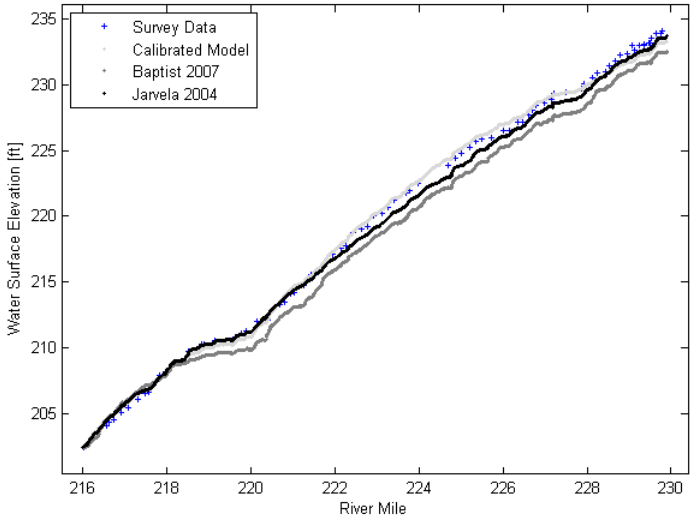

Figure 2 Simulated water surface elevation (ft) as a function of river mile (mi) for Q = 7500 cfs in a reach of the San Joaquin River. Shown for comparison are measured water surface elevation (blue), manually calibrated simulation results (light grey), simulation results using the Baptist (2007) approach (grey), and simulation results using the Jarvela (2004) approach (black). The figure demonstrates that the Jarvela (2004) approach performs better than the Baptist (2007) approach, although falls short of the performance of the manually calibrated model.

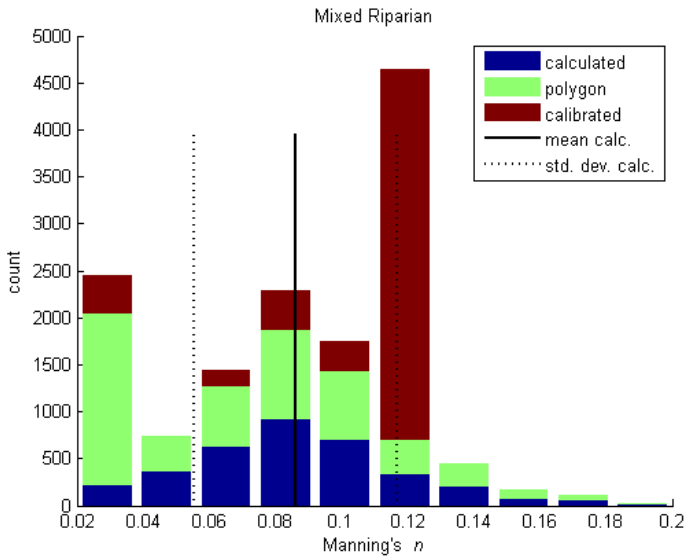

Figure 3 Distribution of Manning's *n* values for Mixed Riparian vegetation in the computational mesh of the modeled reach of the San Joaquin River. Shown in the figure are the calculated values for wetted cells using the Jarvela (2004) approach (blue), the polygon values including those calculated in wet cells and default values in dry cells (green), and the values taken from the manually calibrated model (red). Also shown are the mean (solid line) and standard deviation from the mean (dashed line) of the calculated Manning's *n* values for wetted cells.

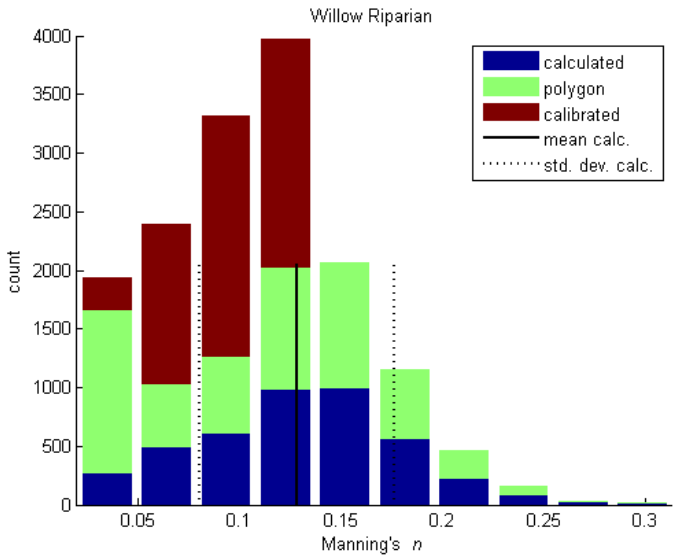

Figure 4 Distribution of Manning's *n* values for Willow Riparian vegetation in the computational mesh of the modeled reach of the San Joaquin River. Shown in the figure are the calculated values for wetted cells using the Jarvela (2004) approach (blue), the polygon values including those calculated in wet cells and default values in dry cells (green), and the values taken from the manually calibrated model (red). Also shown are the mean (solid line) and standard deviation from the mean (dashed line) of the calculated Manning's *n* values for wetted cells.

The comparisons in Figure 1 and 2 show that water surface elevation is underestimated in approximately the upper 2/3 of the model reach using the Jarvela (2004) approach for calculating roughness. This suggests that preferentially increasing the roughness in the upper portion of the model reach may produce simulated hydraulics that better match observed conditions. The mean calculated roughness values for the mixed riparian (Figure 3) and willow scrub (not shown) vegetation types tend lower than the bulk of calibrated roughness values for the same types, which suggests that the spatial distribution of mixed riparian and willow scrub vegetation types may be correlated to the underestimation of water surface elevation in the upper portion of the model reach. Upon inspection of the spatial distribution of mixed riparian and willow scrub vegetation types within the model reach, it is apparent that there is greater spatial coverage in the upper 2/3 of the reach. It was therefore hypothesized that tuning the parameters for the mixed riparian and willow scrub vegetation in order to increase calculated roughness for these types would result in simulated hydraulics that better match the observed conditions. The species-specific drag coefficient C_{dX} was increased from 0.43 to 0.75 for only the mixed riparian and willow scrub types and the model was run again using the Jarvela (2004) approach for calculating roughness. A comparison of water surface elevation for variation in the parameter C_{dX} for a simulated discharge of Q = 7500 cfs is shown in Figure 5. The comparison demonstrates that increasing the species-specific drag coefficient C_{dX} for the mixed riparian and willow scrub vegetation positively affected the simulated hydraulics by preferentially increasing water surface elevation through regions of the modeled reach that were underestimated using a constant value C_{dX}. The variation in parameter C_{dX} resulted in a shift in the distribution of calculated roughness towards larger values. Another test of parameter sensitivity was conducted by varying the exponent X in Equation 2 for the mixed riparian and willow scrub vegetation types. Increasing the fractional exponent X has the effect of increasing roughness, however, with a less than linear sensitivity. For the trial simulation, X was increased from -0.57 to -0.35 for the mixed riparian and willow scrub vegetation types, however the effect on the simulated water surface elevation was small

compared to the effect when varying the drag coefficient, C_{dX}. Comparison of water surface elevation at additional discharges and sensitivity analysis for varying input parameters is provided in Gillihan (2013).

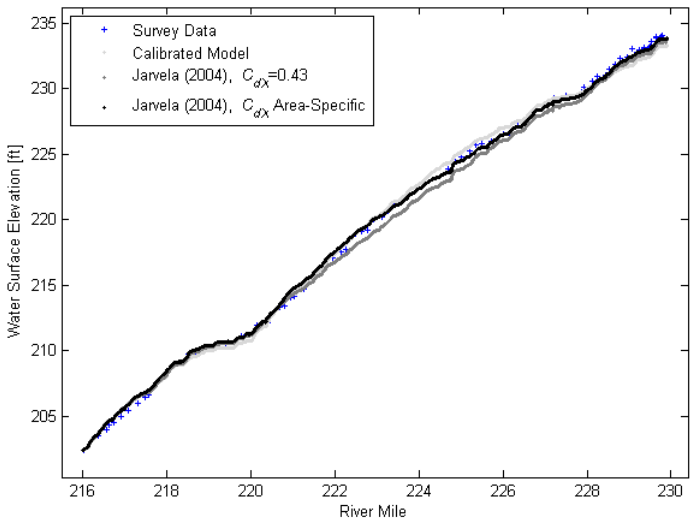

Figure 5 Simulated water surface elevation (ft) as a function of river mile for Q=7500 cfs in a reach of the San Joaquin River. Simulation results are shown for the Jarvela (2004) approach using constant C_{dX}=0.43 (grey) for all vegetation and C_{dX}=0.75 (black) for mixed riparian and willow scrub vegetation. Shown for comparison are measured water surface elevation (blue) and manually calibrated simulation results (light grey). The comparison demonstrates that increasing the species-specific drag coefficient C_{dX} for the mixed riparian and willow scrub vegetation positively affected the simulated hydraulics by preferentially increasing water surface elevation through regions of the modeled reach that were underestimated using a constant value C_{dX}.

DISCUSSION

The results demonstrate that the SRH-2DV model for simulating vegetated flow is generally successful in reproducing the effect of riparian vegetation on water surface elevation as compared to that of measurements and manually calibrated simulations. Distributions of calculated roughness values due to vegetation were generally consistent with values compiled in the literature (Hession & Curran, 2013). The Jarvela (2004) and Baptist (2007) approaches for computing roughness were both implemented in the model. The calibration procedure assumed variables computed by the hydraulic solver (U, h), vegetation characteristics measured in the field (LAI, H, m, D), and parameter values borrowed from published literature (X, U_X) to be known quantities; the parameters C_{dX} and C_d were assumed uncertain and subject to variation.

A likely source of significant error in the modeling is due to limitations imposed by applying locally measured vegetation parameters to spatially disparate zones within the computational mesh. Identical vegetation classes are likely only qualitatively equivalent and so it is predicted that accuracy improvements would be realized by comprehensive measurement of vegetation characteristics throughout the model domain.

The leaf area index is generally a convenient physically-based metric for quantifying vegetal density and area (Jalonen, Jarvela, & Aberle, 2013), and can be estimated by in situ observation or remote sensing. Further, the Jarvela (2004) approach incorporates water depth and velocity information, both of which are directly computed by the hydraulic solver. Given the spatially-detailed information that a two-dimensional hydraulic model can provide, it would be desirable to map measured vegetation parameters at similar scale and resolution (Abu-Aly, Pasternack, Wyrick, Barker, Massa, & Johnson, 2014), which would necessitate the use of remote sensing technologies.

The distributions of calculated roughness values produced by the model and the effect of varying the parameter C_{dX} in Equation 1 indicate that predicting the effects of vegetation on hydraulics is dependent on quantifying complicated species-specific coupling between the vegetation characteristics and local hydraulics. Further exploration of input parameter values and species dependency, a topic of active research (Aberle & Jarvela, 2013), will be useful in gauging applicability and evaluating performance of the algorithms.

Despite the uncertainties identified in the measured and parameterized vegetation characteristics applied in the SRH-2DV model, the simulation results demonstrate good qualitative performance as compared to observed conditions and calibrated results. It is anticipated that the model will serve as a useful tool for predicting the effects of projected vegetation changes and for use as a design tool in restoring riparian vegetation. As the challenges associated with measurement of vegetation characteristics over large spatial scales are overcome through developing remote-sensing techniques, the practicality and accuracy of vegetated-flow modeling will increase.

REFERENCES

Aberle, J., & Jarvela, J. (2013). Flow Resistance of Emergent Rigid and Flexible Floodplain Vegetation. *Journal of Hydraulic Research, 51*(1), 33-45.

Abu-Aly, T. R., Pasternack, G. B., Wyrick, J. R., Barker, R., Massa, D., & Johnson, T. (2014). Effects of LiDAR-derived, spatially distributed vegetation roughness on two-dimensional hydraulics in a gravel-cobble river at flows of 0.2 to 20 times bankfull. *Geomorph.*(206), 468-482.

Baptist, M., Babovic, V., Rodriguez Uthurburu, J., Keijzer, M., Uittenbogaard, R., Mynett, A., et al. (2007). On Inducing Equations for Vegetation Resistance. *Journal of Hydraulic Research, 45*(4), 435-450.

Chow, V. (1959). *Open-Channel Hydraulics*. New York: McGraw-Hill Co.

Darby, S. E. (1999). Effect of Riparian Vegetation on Flow Resistance and Flood Potential. *Journal of Hydraulic Engineering*, 443-454.

Dombroski, D., Greimann, B. P., & Gordon, E. (2012). *Hydraulic Studies for Fish Habitat Analysis.* Denver: Bureau of Reclamation.

Fathi-Moghadam, M., & Kouwen, N. (1997). Non-Rigid, Non-Submerged, Vegetation Roughness in Flood Plains. *Journal of Hydraulic Engineering*, 51-57.

Gillihan, T. (2013). *Dynamic Vegetation Roughness in the Riparian Zone*. Master Thesis, University of New Mexico, Department of Civil Engineering.

Hession, W. C., & Curran, J. C. (2013). The Impacts of Vegetation on Roughness in Fluvial Systems. In J. F. Schroder, D. R. Butler, & C. R. Hupp (Eds.), *Treatise on Geomorphology* (Vol. 12, pp. 75-93). San Diego, CA: Academic Press.

Jalonen, J., Jarvela, J., & Aberle, J. (2013). Leaf Area Index as Vegetation Density Measure for Hydraulic Analyses. *J. Hydr. Eng., 139*(5), 461-469.

Jarvela, J. (2004). Determination of Flow Resistance Caused by Non-Submerged Woody Vegetation. *International Journal of River Basin Management, 2*(1), 61-70.

Jarvela, J. (2005). Effect of Submerged Flexible Vegetation on Flow Structure and Resistance. *Journal of Hydrology*, 233-241.

Kouwen, N., & Fathi-Moghadam, M. (2000). Friction Factors for Coniferous Trees Along rivers. *Journal of Hydraulic Engineering*, 732-740.

Kouwen, N., & Li, R.-M. (1980, June). Biomechanics of Vegetative Channel Linings. *Journal of the Hydraulics Division, Proceedings of the ASCE, 106*(HY6), 1085-1103.

Lai, Y. G. (1997). An Unstructured Grid Method for a Pressure-Based Flow and Heat Transfer Solver. *Numerical Heat Transfer, Part B*, 267-281.

Lai, Y. G. (2000). Unstructured Grid Arbitrarily Shaped Element Method for Fluid Flow Simulation. *AIAA Journal, 38*(12), 2246-2252.

Lai, Y. G. (2010). Two-Dimensional Depth-Averaged Flow Modeling with an Unstructured Hybrid Mesh. *Journal of Hydraulic Engineering, 136*(1), 12-23.

Moise, G. H., & Hendrickson, B. (2002). *Riparian Vegetation of the San Joaquin River*. State of California Department of Water Resources.

Nepf, H. M. (2012). Hydrodynamics of Vegetated Channels. *Journal of Hydraulic Research*, 262-279.

Thompson, G. T., & Roberson, J. A. (1976). A Theory of Flow Resistance for Vegetated Channels. *Transactions of the ASAE*, 288-293.